

# Effects of Ion Implanted C and N on the Sputter Behaviors of Ti and Mo Grid Materials

Paul J. Wilbur, Joshua Miller  
Department of Mechanical Engineering  
Colorado State University  
Fort Collins, CO 80523  
970-491-8564  
pwilbur@engr.colostate.edu

and  
Don L. Williamson  
Department of Physics  
Colorado School of Mines  
Golden, CO 80401  
303-273-3837  
dwilliam@mines.edu

IEPC-01-117

**An experimental study of the effects of ion implantation of nitrogen and carbon into titanium and molybdenum ion thruster grid materials is described. It is suggested that the implantation temperature and current density should be 850 °C and ~2 mA/cm<sup>2</sup>, respectively. It is argued that this will prevent undesirable metallurgical changes, enable relatively rapid processing and produce a balance between the delivery and diffusion of the implanted species. Evidence is offered that C implantation of Ti induces the greatest reduction in sputter yield, but some reduction is observed in all cases. Even though a modest yield reduction is observed when N is implanted into Mo, insignificant levels of N are found in this material.**

## Introduction

As the of ion thruster mission durations increase it becomes more important to have grid materials that resist sputter erosion and thereby enable correspondingly long grid lives. It is desirable to effect this improvement without a substantial increase in the cost of the grids. A possible method of increasing the sputter resistance of grids without introducing new and unproven fabrication techniques could involve conventional fabrication of molybdenum or titanium grids followed by ion implantation processing of the finished products to enhance their sputter resistance.

Evidence that implantation could be effective is suggested by the fact that ambient nitrogen in ion thruster test facilities induced order of magnitude reductions in the sputter yields of molybdenum grids [1,2].

In order to examine the viability of the concept, small coupons of Ti and Mo grid materials (AMS 4901 Ti and pure Mo) were implanted with nitrogen or carbon (as CH<sub>4</sub>) and the changes induced in the coupon properties were studied. Carbon and nitrogen were selected for implantation because these elements generally diffuse readily and form hard precipitates in the metals.

## Apparatus and Procedures

The critical parameters that are controlled during ion implantation using the implant species selected are: 1) the implantation ion current density, 2) the energy of the ions, 3) the implantation time (or dose of ions delivered), and 4) the temperature of the metal coupon during implantation. In the course of this work different equipment was used so these parameters could be varied over wide ranges and preferred values of these parameters and procedures could be established. The ranges of these parameters that were investigated were: current density -- 0.1 to 10 mA/cm<sup>2</sup>, energy -- 1 to 60 keV, and time -- 1 to 9 hours. Coupon temperature was controlled using direct beam heating and/or resistance heating from the unimplanted side. On the basis of these investigations, it was concluded that the processing was most readily accomplished by holding current density fixed at a value of order 2 mA/cm<sup>2</sup> and adjusting the ion energy in the range 2 to 10 keV as necessary to maintain a desired coupon temperature for a prescribed time.

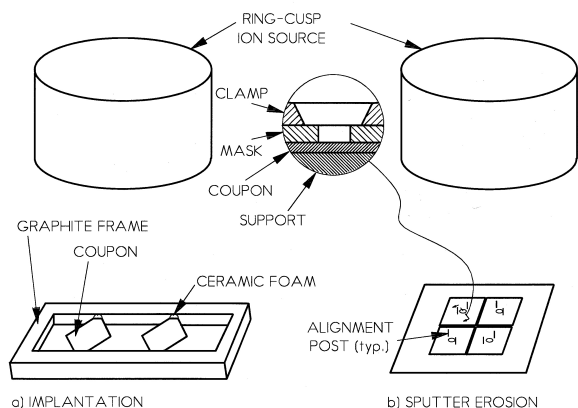


Fig. 1 System Processing Schematics

The final system arrangement selected for the processing is shown schematically in Fig. 1a. The coupons used, which had been polished to 0.01  $\mu\text{m}$  mean roughness on the surface to be implanted, were 0.5 mm thick by 2.5-cm squares. As the figure suggests, the coupons were supported on diagonal corners in a graphite frame that could be opened to insert the corners in ceramic foam insulating buttons. A chromel-alumel thermocouple was spot welded at the center on the back of each coupon so its temperature could be monitored. Several layers of

0.013 mm thick by 2.5-cm square tantalum foil were placed over the unimplanted surface to limit heat losses from it. The frame could be translated to position one coupon in the center of the beam while the other was shielded from it. A 15-cm diameter ring-cusp ion source [3] with SERT II grids [4] that had been masked down to produce a 12-cm beam was used to supply and accelerate the ions.

In order to determine the thermal behavior of a coupon mounted and implanted as described, one was instrumented with three thermocouples (one at the center and one at each of the corners that was not pushed into the foam). When the coupon was heated in a 2.1 mA/cm<sup>2</sup> xenon ion beam, the temperature histories shown in Fig. 2 were measured. The changes in slope seen at times between 200 and 320 sec were each associated with changes made in positive high voltage above or below the nominal value of 2 kV to attain and then maintain a center temperature of 830 °C. It is noteworthy that the difference between the center temperature and those at the two corners may approach as much as 80 °C even though translation of the sample in the beam suggested the incident ion current density was quite uniform over the dimensions of the sample. It is believed that temperatures are lower at the corners because of additional heat radiated from coupon edges and under-edge surfaces that are not shielded effectively by the foil.

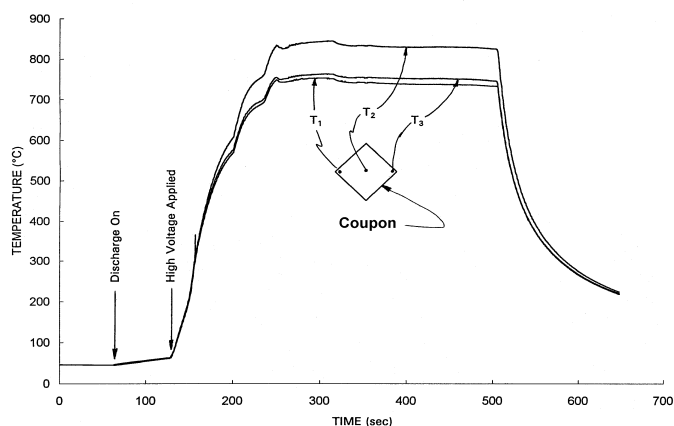


Fig. 2 Implantation Temperature History

After implantation, measurements were made to determine the effects of the treatment. They included sputter yield measurements that involved the test apparatus shown in Fig. 1b. The ion source used for

these measurements was the same as that used for implantation except that small-hole accelerator grids [3] spaced at 0.8 mm were used. The source was operated to produce a 500 eV xenon ion beam which for these tests was generally at a current density in the range between 1.1 and 1.3 mA/cm<sup>2</sup>. Several coupon-holding schemes were used in the study, but the one shown in Fig. 1b was most successful. This scheme involved four coupons centered in the beam that were exposed simultaneously to the beam via 3-mm diameter holes in a 0.5 mm thick mask made of the same material as the coupon. The mask and coupon were clamped between an upper stainless steel plate and a water-cooled copper support plate. The alignment post pairs shown for each coupon enabled removal and replacement so sputter erosion could be accomplished repeatedly in the same crater. It was anticipated that this would make it possible to determine yields as a function of depth.

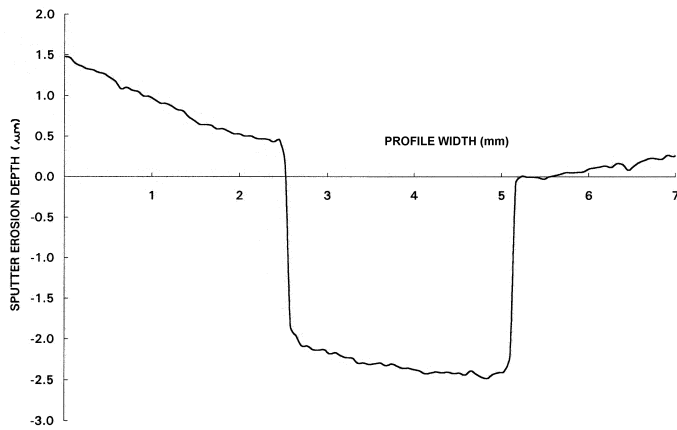


Fig. 3 Typical Profilometer Trace of Crater

After exposure to the beam through the mask the coupons were removed and the steps at the edges of the sputter eroded craters like the one shown in Fig. 3 were measured using a Talysurf 10 profilometer. In order to obtain reliable mean values of the crater depth, three profilometric traces oriented 120° apart were taken across each crater and several measurements of the distance between a reference surface line and the bottom of the crater were made across each trace. Sputter yields were computed using:

$$Y = \frac{\rho_g d N_A e}{M_g j t} \quad (1)$$

where  $\rho_g$  and  $M_g$  are the density and molecular mass of the grid material,  $d$  is the mean depth of the erosion crater,  $N_A$  is Avagadro's number,  $e$  is the electron charge,  $j$  is the ion current density and  $t$  is the erosion time.

The effectiveness of implantation was measured indirectly by cross-sectioning implanted samples, mounting them, polishing the sectioned edge, and then measuring the Vicker's microhardness as a function of depth (i.e. across the edge). Typically, three indentations were made using an indenter load of 3 gm and a dwell time of 10 sec to obtain a data point for plotting at each depth. The nominal standard deviation associated with these measurements was about 15 kg/mm<sup>2</sup>.

Changes in the microstructure of the grid materials induced by implantation were determined using X-ray diffraction (XRD) in the standard Bragg-Brentano geometry with Cu K $\alpha$  radiation. This instrument senses microstructures in a region that extends about 1  $\mu$ m beneath the surface.

### Processing Temperature Considerations

The approximate depth  $\langle x \rangle$  to which implanted ions will diffuse in a time  $t$  is given by

$$\langle x \rangle = \sqrt{D_0 t} \exp\left(\frac{-E}{2 k T}\right) \quad (2)$$

where  $D_0$  is the diffusion coefficient prefactor,  $E$  is the material-and-implant-ion-dependent activation energy for diffusion,  $k$  is Boltzmann's constant and  $T$  is the temperature that prevails during the implantation. This equation shows it is important to have a temperature that is as high as possible to reduce the diffusion time and, hence, the cost of processing.

Ando, et al. [5] reported that temperatures in the range 900 to 1100 °C yielded nitrogen diffusion to depths of 100  $\mu$ m in Ti after only several minutes of nitriding with a plasma jet. On the basis of their results this temperature range was accepted as a reasonable starting temperature for the study.

## Results

When either N or C was implanted at temperatures near 1100 °C it was found that the Ti coupon was badly distorted and both the Ti and Mo coupons had become brittle. Either condition was considered unacceptable for a grid processing application. The causes of these undesirable effects were traced to a Ti phase change from close-packed hexagonal to body-centered cubic that occurs near 885 °C [6] and brittleness that appeared to be related to grain growth that begins to occur near the minimum recrystallization temperature for Mo (900 °C [6]). Since these temperatures are sensitive to impurities some margin against the transformations was considered necessary and 850 °C was selected as an upper limit for the processing.

### Hardness Profiles

The effect of nitrogen implantation on the hardness profile through a Ti coupon from the implanted side (at zero) toward the unimplanted one is found in Fig. 4. It shows the unimplanted material with a hardness near 255 H<sub>v</sub> (Vicker's units) and values over twice that at the edge that had been implanted with nitrogen. The hardness profiles are also observed to rise as the implantation time is increased from 1 to 9 hours. The data shown extend only to 150 μm but measured hardnesses remained constant near 360 H<sub>v</sub> for the 9-hr curve and near 255 H<sub>v</sub> for the others all the way to the unimplanted surface. Each of the data points shown is the mean of ten hardness measurements, which typically exhibited a ±15 H<sub>v</sub> standard deviation. It is argued that hardness increases are indicative of increased nitrogen content, which is in turn indicative of improved sputter resistance. The nitrogen delivered to the surface during the 9-hr treatment is sufficient to leave 20 at. % nitrogen throughout the coupon thickness.

When carbon was implanted for the same times, the data of Fig. 5 were obtained. These data also show that carbon implantation induces an increase in hardness from the implanted surface to a depth that increases with implantation time. In the case of the sample implanted for 9 hours, a modest but significant increase in hardness can be seen at its midpoint thickness (~250 μm), but diffusion does not appear as effective as it was for implanted nitrogen.

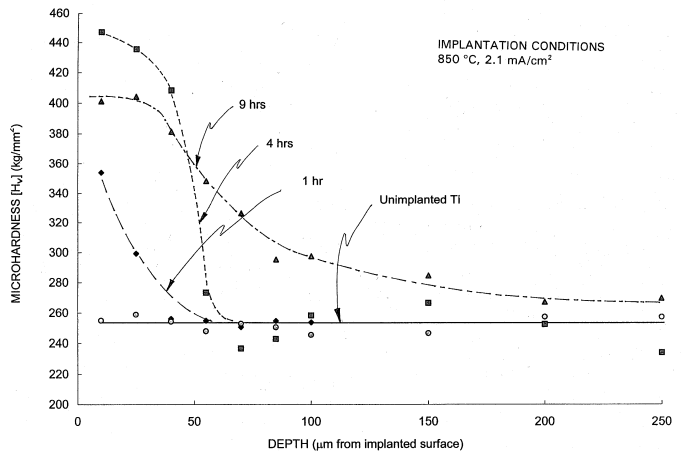


Fig. 4 Effect of N Implantation Time on Ti Coupon Microhardness Depth Profile

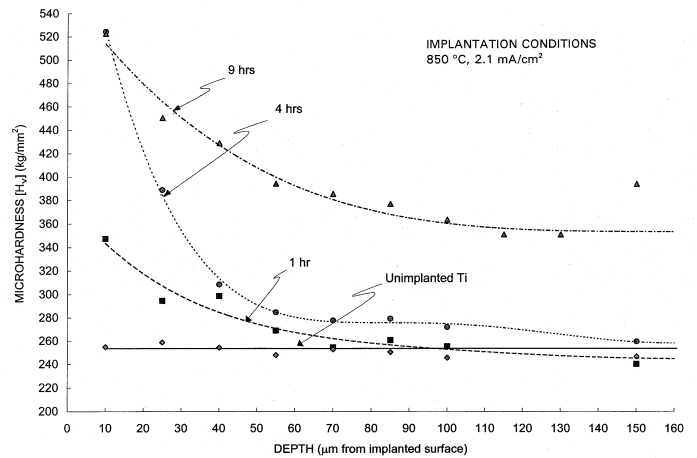


Fig. 5 Effect of C Implantation Time on Ti Coupon Microhardness Depth Profile

A possible reason for a lower rate of carbon diffusion is related to the relative rates of carbon diffusion from the region being implanted and carbon delivery to it via the ion beam. Carbon diffusion in this situation is complicated because: 1) the diffusion rate exhibits the usual exponential sensitivity to temperature, 2) temperatures near 850 °C are required to enable carbon diffusion at nominal implantation rates, 3) heat loss from the surface being implanted occurs primarily via radiation, and 4) carbon accumulation on the implanted surface induces an increase in its radiative emissivity. Hence, slight carbon accumulation on the surface increases radiative losses, causes the surface temperature to drop thereby inhibiting carbon diffusion

and enhancing the rate of carbon accumulation on the surface even further. Once the carbon accumulation reaches a few nanometers, implanted carbon ions come to rest in the carbon coating rather than the metal and the benefits of carbon delivery via implantation are lost.

During processing of the coupons for Fig. 5, temperature was controlled by increasing the implantation energy and it was necessary to increase this energy continuously during the processing. Marginal carbon accumulation on Ti coupon surfaces at the conditions of Fig. 5 is suspected to have necessitated the energy increases. This suspicion was strengthened by evidence of surface discoloration and the fact that hardnesses measured on a coupon implanted for 1 hr at a lower current were greater and extended deeper into the material than the 1-h data of Fig. 5.

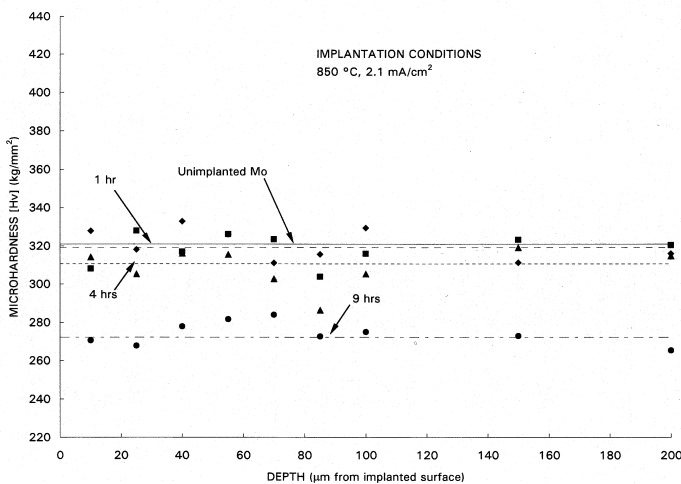


Fig. 6 Effect of N Implantation Time on Mo Coupon Microhardness Depth Profile

The effects of nitrogen and carbon implantation into molybdenum on hardness profiles are shown in Figs. 6 and 7. Both of these profiles are markedly different that those for with Ti coupons. They show no significant hardness variation with depth (mean values were the same through the full 500 µm coupon thickness) and that both Mo coupons are softened significantly after 9 h of implantation. The 1-hr data in Fig. 7 do suggest carbon implantation induces a modest hardness increase if the processing time is not too long.

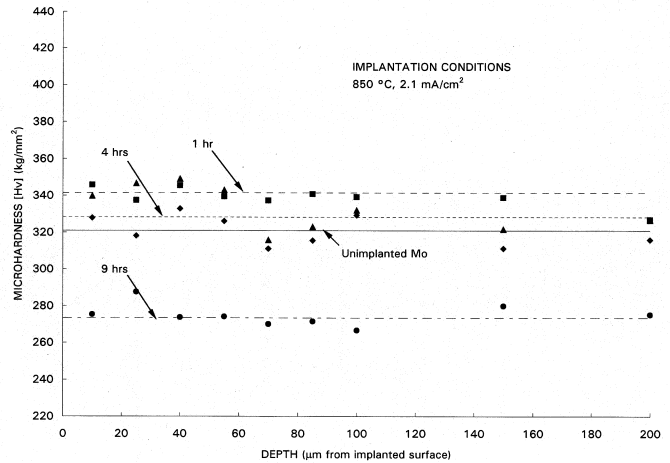


Fig. 7 Effect of C Implantation Time on Mo Coupon Microhardness Depth Profile

### X-ray Diffraction Analysis

X-ray diffraction (XRD) patterns for Ti coupons implanted with N and C at 850 °C are shown in Figs. 8 and 9 along with stick diagrams that indicate the angular positions and relative strengths of diffraction peaks associated with pure elements and the compounds that might be expected. The square root of x-ray intensity is plotted to reveal more clearly any weaker peaks due to secondary phases. From Fig. 8 it is observed that peak patterns are about the same for all three implantation times. This suggests that the near-surface ( $\approx 1 \mu\text{m}$ ) composition develops and stabilizes within an hour. By comparing stick-figure and measured peaks it is concluded that significant amounts of Ti, TiN and  $\text{Ti}_2\text{N}$  are all present. It is noted that two references giving data for  $\text{Ti}_2\text{N}$  were found and the data designated  $\text{Ti}_2\text{N}^*$  (tetragonal, JCPDS-File No. 17-0368 [7]) rather than those designated  $\text{Ti}_2\text{N}^{**}$  (tetragonal, JCPDS-File No. 23-1455 [7]) were found to give a better match to the measured results.

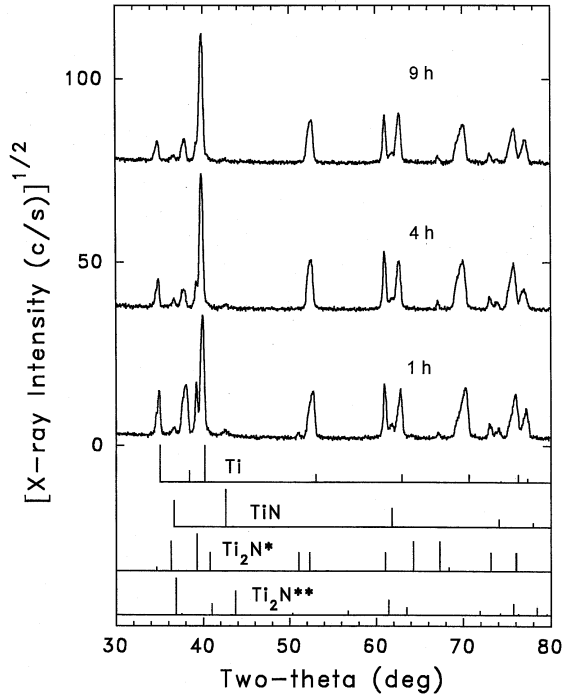


Fig. 8 Effect of N Implantation Time on Ti Coupon X-ray Diffraction Pattern

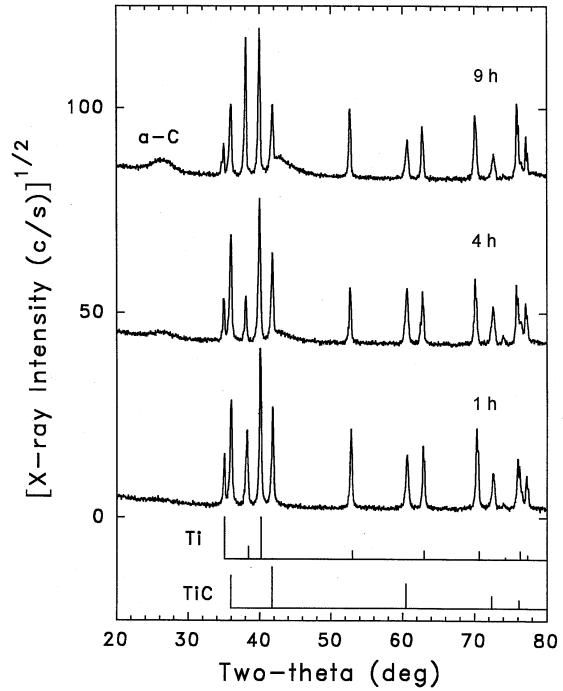


Fig. 9 Effect of C Implantation Time on Ti Coupon X-ray Diffraction Pattern

Figure 9 shows measured data for the C-implanted Ti coupons and stick diagrams for Ti and its carbide, TiC. Comparison of the measured diffraction peaks with the stick diagram peaks reveals that both Ti and TiC are present. The coupon implanted for 9 h shows clear evidence of a broad amorphous carbon (a-C) peak near  $26^\circ$ . Its presence strengthens the hypothesis that carbon accumulates on the surface during implantation and eventually inhibits the diffusion of incident carbon. Figure 10 indicates that Mo and  $\alpha$ -phase  $\text{Mo}_2\text{C}$  are the dominant phases formed when C is implanted into Mo although a small amount of  $\gamma$ -phase MoC is formed under some conditions. Hence, carbides are present even though the hardness data seem not to reflect it.

The XRD patterns measured on the same unimplanted Mo grid material as that implanted with N at  $2.1 \text{ mA/cm}^2$  and  $850^\circ\text{C}$  are compared with the idealized, published spectrum for randomly oriented pure Mo grains in Fig. 11. The numbers on the stick diagram (JCPDS-File No. 42-1120 [7]) are the Miller indices associated with the various crystallographic planes that induce the peaks. They suggest N

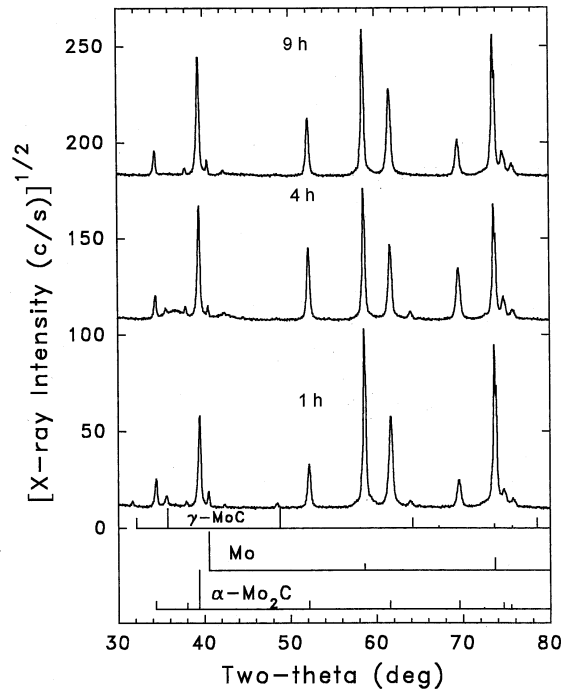


Fig. 10 Effect of C Implantation Time on Mo Coupon X-ray Diffraction Pattern

implantation causes plane reorientation, which changes relative peak strengths, but there is no evidence of any new peaks that might be associated with nitride precipitates. There are also no observable differences in peak position and this indicates the material contains no N in solid solution. It is observed that the grain reorientation mentioned in the preceding paragraph could be caused by preferential sputtering and/or grain growth or modification during the time a coupon is at high temperature. Finally, it is noted that nitrides were sensed at substantial concentrations when implantation was carried out at lower temperatures (500 and 600 °C) but the hardening effect appeared to be modest in that temperature range as well.

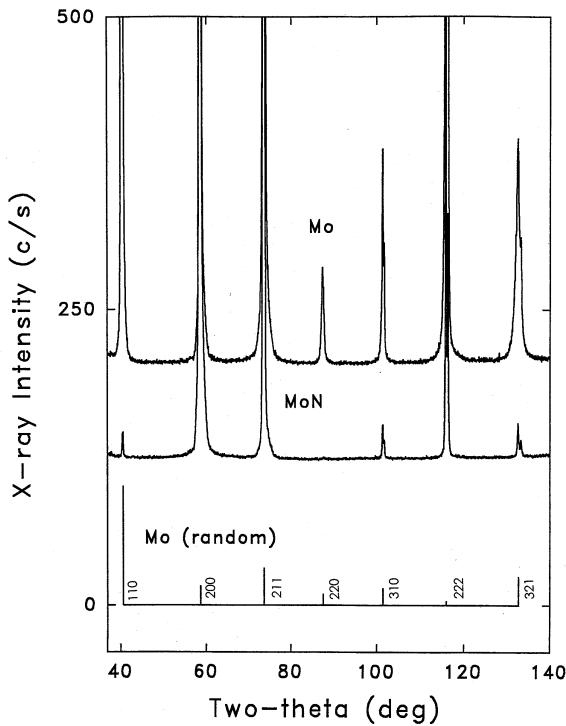


Fig. 11 X-ray Diffraction Pattern Comparison of N Implanted and Unimplanted Mo Coupons

### Sputter Yield Measurements

Measurements of 500-eV, xenon sputter yields made on molybdenum and titanium coupons implanted with either carbon or nitrogen for times that ranged between 1 and 9 hours are shown in Fig. 12. The yield data in this figure have been normalized by dividing them by yields measured for corresponding unimplanted Ti and

Mo coupons. These unimplanted yields were typically several percent lower than published values, which are  $\sim 0.88$  atoms/ion for Mo and  $\sim 0.44$  atoms/ion for Ti [8]. The data of Fig. 12 show that: 1) sputter yields decrease as the duration of the implantation is increased, 2) carbon implantation into titanium induces the greatest reduction in sputter yield ( $\sim 55\%$ ) and 3) nitrogen implantation into molybdenum induces the smallest reduction ( $\sim 15\%$ ). Although these data are mean yields to depths of a few microns from the surface, it is argued that hardness increases to greater depths suggest the yields are depressed to these deeper depths also. Attempts to measure sputter yields to greater depths by repeatedly sputtering and measuring erosion depths in the same craters were frustrated by difficulties in obtaining reproducible results.

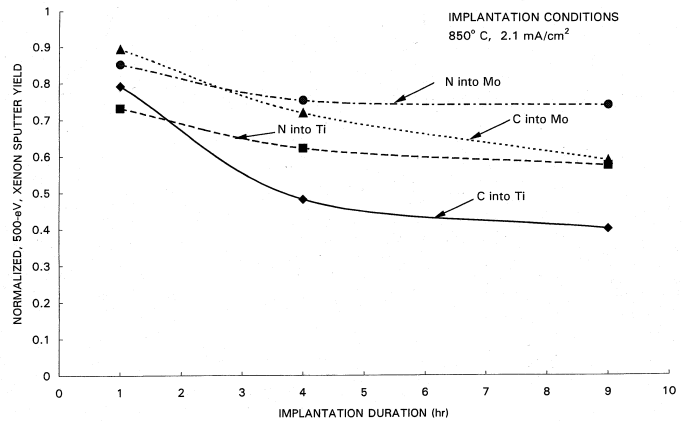


Fig. 12 Effect of Implantation Time on Normalized Sputter Yields

### Discussion

Implantation of nitrogen into Ti causes the hard precipitates  $TiN$  and  $Ti_2N$  to form. It is known that they are precipitates rather than a continuous layer because the Ti peaks would be much weaker or absent if the layer was continuous. The nitrogen diffuses quite readily at  $850^\circ C$  and in 9 hours induces a hardness increase through the nominal thickness of grids that are typically used in low specific impulse applications ( $500 \mu m$ ). The hardness increase through the coupon is also a reflection of precipitate rather than continuous layer formation.

Carbon implanted into Ti results in the precipitation of  $TiC$  and yields the most sputter resistant material of

those investigated. After 9 hrs of implantation at 850°C, hardness measurements indicate carbon also diffuses through a 500- $\mu\text{m}$  thick coupon although the incremental hardness increase at the unimplanted surface was less than it was for the N-implanted one. It is anticipated that hardnesses and treatment depths could be improved by reducing the C implantation current density so a better balance between the carbon implantation and diffusion rates existed. This should prevent C accumulation on the implanted surface.

Both the XRD and hardness profile data indicate that nitride formation in and solid solution strengthening of Mo are insignificant when N is implanted into it at 850 °C. It is argued that this situation develops because molybdenum nitrides are unstable and nitrogen solubility in Mo is very low at this temperature (<10 ppm) [9]. Sufficient nitrogen was supplied in 9 h to induce a high concentration throughout the coupon (>20 atom %) but these conditions coupled with a modest diffusion rate [9] suggest all of the implanted N escaped back out of the surface being implanted.

The decrease in hardness induced by N implantation of Mo is almost certainly related to recrystallization of cold worked grains in this material. This process involves initial formation of small grains in the cold worked material which soften it. Even though temperatures were kept below the minimum recrystallization temperature during processing, it is considered likely that the longest (9 h) processing time was sufficient to induce the growth of the small grains that produce this effect.

The hardness data indicate that the recrystallization process also occurs when C is implanted into Mo. In this case, however, carbides form and the flatness of the hardness profile suggests that the C either diffuses rapidly or much of it is lost back out of the implanted surface.

It is noted that the beneficial sputter-impeding effects of nitrogen could probably be made available if its solubility in Mo could be increased. It might be possible to do this by alloying the molybdenum with an appropriate element such as Cr, which is known to have enabled an increase in the solubility of nitrogen in stainless steel [10].

Finally, it is noted that some coupon warping occurred during processing even when temperatures were maintained at 850 °C. This is to be expected when precipitates and/or solid solutions are being formed near one surface of a substrate and not at the other because their formation typically results in a localized volume change. Tests were conducted that showed the warpage could be reduced substantially by implanting first one side and then the other. If full-size ion thruster grids are treated it is recommended that they be implanted simultaneously from both sides to mitigate this problem and to achieve greater uniformity of the implanted species in the material.

## Conclusions

Suitable nominal conditions for implantation of Ti grid material with N are a temperature of 850 °C, a current density near 2 mA/cm<sup>2</sup> and energies adjusted around 2 keV as necessary to maintain the temperature. After 9 h of such treatment there is evidence that N diffusion to a depth of 0.5 mm has occurred and that the near-surface sputter yield has decreased by 35%.

The nominal conditions are also suitable for C implantation into Ti although a slightly lower current density is preferred to prevent C accumulation on the implanted surface. A similar diffusion depth and a greater near-surface sputter yield reduction (55%) are observed.

Although there is evidence that N and C implantation of Mo reduces its sputter yield at the nominal conditions the reductions are less than they were for implanted Ti. There is no evidence that N diffuses into the Mo and hardens the surface at the selected processing temperature of 850 °C.

## Acknowledgement

Financial support under Research Grant NAG3-1801 through the NASA Glenn Research Center is gratefully acknowledged.

## References

- [1] Rawlin, V.K. and M.A. Manteniaks, "Effect of Facility Background Gases on Internal Erosion of the 30-cm Hg Ion Thruster," AIAA Paper 78-665, 13<sup>th</sup> International Electric Propulsion Conference, San Diego, CA., 1978.
- [2] Garner, C.E., J.R. Brophy, L.C. Pless and J.W. Barnett, "The Effect of Nitrogen on Xenon Ion Engine Erosion," AIAA Paper 90-2591, 21<sup>st</sup> International Electric Propulsion Conference, Orlando, FL, 1990.
- [3] Wilbur, P.J. and B.W. Buchholtz, "Surface Engineering using Ion Thruster Technology," AIAA Paper 94-3235, p. 2, 30<sup>th</sup> Joint Propulsion Conference, Indianapolis, IN 1994.
- [4] Kerslake, W.R. D.C. Byers and J.F. Staggs, "SERT II Experimental Thruster System," AIAA Paper 67-700, Electric Propulsion Conference, Colorado Springs, CO, 1967.
- [5] Ando, Y., S. Tobe, H. Tahara and T. Yoshikawa, "Effects of Addition of Hydrogen to Nitrogen Plasma during Nitriding of Titanium and SACM645 Steel Using Supersonic Expanding Nitrogen Plasma Jets," IEPC Paper 99-201, 30<sup>th</sup> International Electric Propulsion Conference, Kitakyushu, Japan, 1999.
- [6] *Metals Handbook*, J.R. Davis ed., ASM International, v. 2, 10<sup>th</sup> Ed, pp. 574, 1140 & 1169, 1990.
- [7] Holmberg, *Acta Chem. Scand.*, v.16, p.1255, 1962.
- [8] Wehner, G.K., "Sputter Yield Data in the 100-600 eV Energy Range," General Mills Report 2309, July 15, 1962. 10.
- [9] Evans, J.H. and B.L. Eyre, "The Heat of Solution and Diffusivity of Nitrogen in Molybdenum," *ACTA Metallurgia*, v. 17, pp. 1109-1115, 1969.
- [10] Williamson, D.L., O. Ozturk, R. Wei and P.J. Wilbur, "Metastable phase formation and enhanced diffusion in f.c.c. alloys under high dose, high flux nitrogen implantation at high and low ion energies," *Surface and Coatings Technology*, v. 65, p. 15, 1994.